Remote control of the retroflection of the Labrador Current

Mathilde Jutras (mathilde.jutras@mail.mcgill.ca)
McGill University https://orcid.org/0000-0001-5154-5009
Carolina Dufour
McGill University https://orcid.org/0000-0002-1441-3880
Alfonso Mucci
McGill University https://orcid.org/0000-0001-9155-6319
Lauryn Talbot
McGill University

Article

Keywords:

Posted Date: January 31st, 2023

DOI: https://doi.org/10.21203/rs.3.rs-2045201/v1

Additional Declarations: There is **NO** Competing Interest.

Version of Record: A version of this preprint was published at Nature Communications on May 6th, 2023. See the published version at https://doi.org/10.1038/s41467-023-38321-y.

Remote control of the retroflection of the Labrador Current

Mathilde Jutras[1], Carolina O. Dufour[2], Alfonso Mucci[1,3], and Lauryn Talbot[2]

[1]*Department of Earth and Planetary Sciences, McGill University, Montreal, QC, Canada*
[2]*Department of Atmospheric and Oceanic Sciences, McGill University, Montreal, QC, Canada*
[3]*Geotop, Université du Québec à Montréal, Montreal, QC, Canada*

Abstract

The Labrador Current carries cold, relatively fresh, and well-oxygenated waters into the subpolar North Atlantic and into the Slope Sea. The relative contribution of these waters to either region depends on the eastward retroflection of the Labrador Current at the Grand Banks. We develop a retroflection index based on virtual Lagrangian particles and show that the amplitude of the retroflection is mostly controlled remotely by large-scale forcing, related to winds over the Labrador Shelf and to subpolar gyre dynamics, whereas eddies and meanders arising from interactions between the Labrador Current and the Gulf Stream play a secondary role. The mechanistic understanding of the drivers of the Labrador Current retroflection should help to predict changes in the water properties of both export regions, and anticipating their important consequences on marine life and deep-water formation.

1 Introduction

Over the last decades, the Slope Sea and northeastern American continental shelf have experienced an increase in water temperatures and a decrease in oxygen concentrations (*Chen et al.*, 2020; *Claret et al.*, 2018; *Petrie and Drinkwater*, 1993, among others), including in connected bodies of water such as the St. Lawrence Estuary (*Jutras et al.*, 2020; *Gilbert et al.*, 2005) and the Gulf of Maine (*Whitney et al.*, 2022; *Pershing et al.*, 2016), with dire consequences on marine ecosystems (*Poitevin et al.*, 2019; *Chabot and Dutil*, 1999) and fisheries (*Pershing et al.*, 2016; *Mills et al.*, 2013). From 2012 to 2016, the subpolar North Atlantic experienced a strong freshening (*Holliday et al.*, 2020), with potential impacts on the Atlantic meridional overturning circulation (AMOC, *Holliday et al.*, 2020; *New et al.*, 2021). Both the deoxygenation and temperature increase over the shelf as well as the freshening of the subpolar Atlantic have been attributed to an increased export of Labrador Current Water towards the subpolar North Atlantic, at the expense of the Slope Sea and the eastern American continental shelf (*Jutras et al.*, 2020; *Holliday et al.*, 2020).

Originating from the subarctic, the Labrador Current carries cold, relatively fresh, and well-oxygenated waters southward along the Labrador Shelf (Fig. 1). The Labrador Current is characterized by two branches: an inshore branch that flows on the Labrador Shelf, and an offshore branch that flows along the Labrador shelf-break. Near the tip of the Grand Banks, the current splits: part of the current retroflects northeastward to join the North Atlantic Current (NAC), and part continues along the shelf to the west (*Stendardo et al.*, 2020; *Fratantoni and McCartney*, 2010; *Fratantoni and Pickart*, 2007; *Wang et al.*, 2015; *Wu et al.*, 2012; *Luo et al.*, 2006; *Fischer and Schott*, 2002; *Pickart et al.*, 1997, Fig. 1). This area lies at the confluence of the subtropical and subpolar gyres, and hence at the meeting point between the Gulf Stream (or North Atlantic Current, NAC) and the Labrador Current. Though of key importance to the circulation and water properties of the northwestern Atlantic, the retroflection of the Labrador Current and its drivers are still poorly understood (*Fratantoni and McCartney*, 2010).

It has been proposed that the retroflection of the Labrador Current is forced either remotely, upstream of the retroflection point, or locally, at the tip of the Grand Banks. In the remote hypothesis, the retroflection would be controlled by the wind patterns over the Labrador Shelf (*Holliday et al.*, 2020; *Peterson et al.*, 2017) and by the strength of the Labrador Current (*Jutras et al.*, 2020; *Han et al.*, 2019; *Pickart et al.*, 1999). This hypothesis is supported by observations that changes in the amount of Labrador Current Water intrusion into the Slope Sea precede meridional shifts of the Gulf Stream *Peña-Molino and Joyce* (2008). It has also been suggested that a weak Labrador Current retroflection is concurrent with a strong North Atlantic Oscillation (NAO, *Luo et al.*, 2006; *Pershing et al.*, 2001) and AMOC (*New et al.*, 2021; *Saba et al.*, 2016). In contrast, several studies invoked a local control of the retroflection via interactions with the Gulf Stream, either through a northern shift of the Gulf Stream forcing the Labrador Current to retreat (*New et al.*, 2021; *Claret et al.*, 2018; *Urrego-Blanco and Sheng*, 2012), or through interactions with Gulf Stream/NAC eddies and meanders diverting the Labrador Current offshore (*Townsend et al.*, 2015; *Carr and Rossby*, 2001) or blocking the inflow of the Labrador Current towards the Scotian Shelf (*Neto*, 2021; *Zhang et al.*, 2016). Seasonal stratification in the Grand Banks region would also affect the export of freshwater away from the shelf (*Fratantoni and McCartney*, 2010).

We present evidence that remote large-scale forcings drive the retroflection of the Labrador Current, whereas local interactions with eddies and meanders at the tip of the Grand Banks, generated by the presence of the Gulf Stream, only play a secondary role. To do so, we introduce a retroflection index that characterizes the magnitude of the retroflection of the Labrador Current over the past 25 years. This index allows us to examine directly the link between the observed oxygen, temperature and salinity anomalies in the Labrador Current Water export zones, with regard to the retroflection of the Labrador Current, as well as to investigate the link between the retroflection and multiple possible drivers.

2 Results

2.1 Retroflection of the Labrador Current

We examine the retroflection of the Labrador Current from Lagrangian tracking experiments where virtual particles are tracked using velocity fields of the ocean reanalysis GLORYS12V1, over the period 1993 to 2018 (see Method section). The circulation and volume transport, as well as the retroflection, are also studied from an Eulerian perspective for comparison, and presented in supplementary material B. The trajectories of the virtual particles reveal that, from the Grand Banks, the Labrador Current predominantly follow a seesawing system composed of two branches: a westward branch feeding the Slope Sea and the eastern American continental shelf that accounts for about

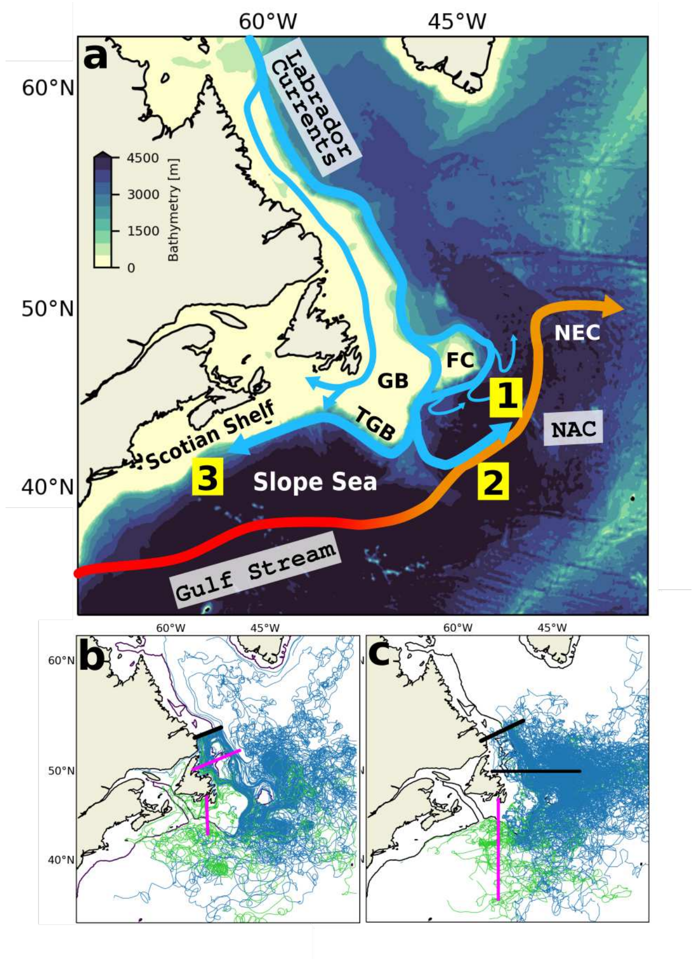

Figure 1: **(a)**: Schematic of the ocean circulation in the region of interest. The background color shows the bathymetry of the GLORYS12V1 model. The thick colored arrows indicate the approximate location of the main currents in the area, with NAC referring to the North Atlantic Current. In this paper, we consider the shelf and shelf-break branches of the Labrador Current together and refer to them as the Labrador Current. Numbers indicate the main pathways of the Labrador Current in the Grand Banks area, as revealed by the trajectories of the virtual particles: (1) diverted eastward between Flemish Cap and the tip of the Grand Banks, (2) diverted eastward at the southern tip of the Grand Banks, and (3) following a western route along the shelf-break. (1) and (2) represent two pathways of retroflection. The following topographic features are indicated: Grand Banks (GB), Tip of the Grand Banks (TGB), and Flemish Cap (FC). NEC refers to the Northeast Corner. **(b)**: Examples of virtual particles trajectories. The thick black line marks the section along which the Lagrangian particles were initialized, and the pink lines the hydrographic sections used to calculate the retroflection index (see section 4.3). **(c)**: Trajectories of Argo, RAFOS/SOFAR floats, and surface drifters over 2000-2018. We select floats that cross the two black lines, and classify them into retroflected or not according to whether they cross the pink vertical line. In (b) and (c), the particles, floats and drifters classified as retroflection appear in blue, and those classified as westward-flowing appear in green. The thin black line delineates the 350-m isobath.

a quarter of the Labrador Current transport downstream of the Grand Banks over 1993-2015, and an eastward branch (the retroflected branch) joining the NAC that accounts for about 60% of the transport. The rest of the particles follow minor pathways that are described in detail in *Jutras et al.*, *In Prep*. The retroflection occurs mostly between Flemish Cap and the tip of the Grand Banks, as well as at the tip of the Grand Banks (respectively ∼25% and ∼30% of the particles leaving the shelf, Fig. 2). These locations coincide very well with the observed leaking points of the Deep Western Boundary Current along the Labrador Shelf (Fig. 3a from *Solodoch et al.*, 2020; *Mertens et al.*, 2014). The pathways of the virtual particles and their relative importance are overall in good agreement with what is observed from the trajectories of surface drifters, Argo and RAFOS/SOFAR floats (Fig. 1 and supplementary material C).

We evaluate the variability of the retroflection of the Labrador Current over 1993-2015 with an index counting retroflected virtual particles (Fig. 1a and 3; see the Method section). The index is very well-correlated with temperature and salinity in the subpolar North Atlantic, in the Slope Sea, and over the northeastern American Shelf (correlation coefficient > 0.6, $p < 0.001$, Fig. 4a), further confirming the seesawing nature of the system and the influence of the Labrador Current in these regions. A strong (weak) retroflection is associated with positive (negative) salinity and temperature anomalies in the Slope Sea and along the Scotian Shelf, and to negative (positive) salinity anomalies in the subpolar North Atlantic (Fig. 3 and 4a). The freshwater input by the Labrador Current towards the subpolar North Atlantic is concentrated in the region east of the Northwest Corner, north of ∼50°N, and then spreads east with the NAC (Fig. 4a, *Pérez-Brunius et al.* (2004); *Fischer and Schott* (2002)). In the Slope Sea, the salty, warm, poorly-oxygenated Gulf Stream waters are found to penetrate adjacent channels such as the Laurentian Channel (Fig. 4a). Quantitatively, an increase in the retroflection index by 1-σ decreases the salinity in the subpolar North Atlantic by 0.10, and increases the salinity in the Slope Sea and close to the Scotian shelf by 0.05. The additional freshwater in the North Atlantic may enhance the water column stratification and interfere with convection (*Böning et al.*, 2016), with implications for the large-scale circulation.

The retroflection index shows a strong multiannual variability: it exhibits a standard deviation of 22% over 1993-2015 (Fig. 3). The retroflection is significantly weaker than the mean state in the 1996-1999 period, and significantly stronger in the 2011-2014 period. The strong retroflection period of 2011-2014 is concurrent with an intense freshening event of the subpolar North Atlantic observed over 2012-2016 (*Holliday et al.*, 2020), with temperature record highs on the eastern American continental shelf (*Chen et al.*, 2020), and a decrease in the inflow of Labrador Current Waters into the Laurentian Channel after 2008 (*Jutras et al.* (2020), see supplementary figure S12c). Our findings are also consistent with float observations which show that more Argo and RAFOS/SOFAR floats carried by the Labrador Current were retroflected in 2009 and 2012-2014 compared to other years (supplementary figure S12). The weak retroflection period of 1996-1999 is concurrent with high salinities in the subpolar North Atlantic reported over the same period (Fig. 3 and *Holliday et al.*, 2020). Overall, observations support the validity of our retroflection index and confirm the role of the Labrador Current dynamics in the 2012-2016 subpolar North Atlantic extreme freshening event (*Holliday et al.*, 2020).

Finally, the retroflection index also exhibits a significant positive trend of +2.4%/decade, equivalent to ∼10% of the inter-annual variability of the index (Fig. 3). After removing this trend, the index still exhibits a number of prolonged periods of weak and strong retroflection exceeding ±1-σ from the mean (highlighted in red and green, respectively, in Fig. 3). This highlights that the strong retroflection period of 2011-2014 is exacerbated by the trend.

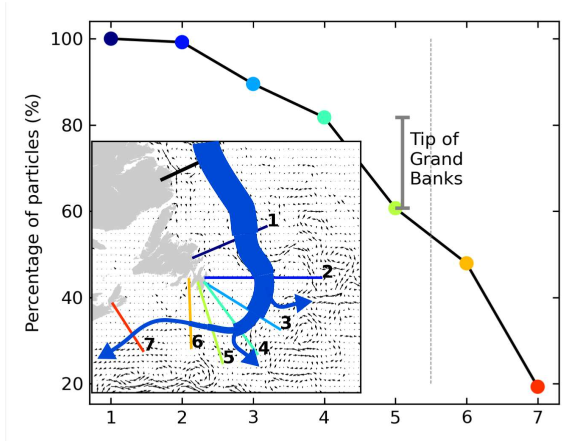

Figure 2: Percentage of the total number of particles that cross each hydrographic section (x-axis) identified in the inset for the 1994–2015 time period. Recirculating particles are counted only once. The vertical bar indicates the loss at the tip of the Grand Banks. Inset: The Labrador Current is represented in blue, and its volume transport is indicated by its width. The arrows illustrate the progressive loss (i.e., leaking points) of Labrador Current Waters. Beyond section 5 (indicated by the vertical dashed line), particles are not counted as retroflected when they leak out of the Labrador Current.

2.2 Remote forcing

We identify a number of forcing mechanisms that appear to play a role in controlling the magnitude of the Labrador Current retroflection. A stronger current is generally associated with a stronger retroflection, as suggested by the positive correlation between the Labrador Current volume transport on the Labrador Shelf and the detrended retroflection index (correlation coefficient of 0.52, $p<0.001$; Fig. 3). This relation advocates for a remote, more specifically upstream, control of the retroflection of the Labrador Current. The correlation is highest for an 11-month lag, approximately the time required for the Labrador Current Water to travel from 52°N on the Labrador Shelf to the tip of the Grand Banks (supplementary material D). The correlation is negative when considering the volume transport downstream of the Grand Banks, on the Scotian Shelf (Fig. 3). This confirms that as more water is diverted to the east, less feeds the Scotian Shelf current (*Han et al.*, 2019). The connection between the Labrador and the Scotian shelves is further supported by significant lagged-correlations of temperature and surface salinity along streams of the Labrador Current (supplementary figure S7). As the Labrador Current forms the western limb of the subpolar gyre, we expect a link between the retroflection and the state of the gyre. We find a significant anti-correlation between the retroflection index and the extent of the subpolar gyre (correlation coefficient of -0.36, $p < 0.0001$; Fig. 3f, see Method section). Since a contracted (i.e. less extended) gyre is associated with a faster circulation of its peripheral currents, this relation implies that the retroflection is typically higher when the gyre is stronger (faster).

In addition to the Labrador Current's strength, the wind, including upstream of the retroflection, also appears to influence the magnitude of the retroflection. Periods of strong retroflection are

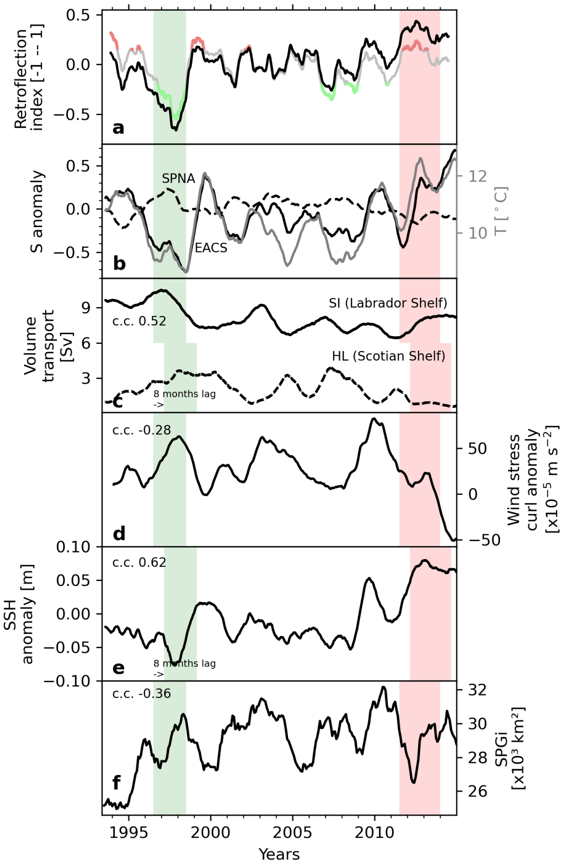

Figure 3: **(a) Retroflection index**: Total (black) and detrended (grey) indices with periods of strong (red) and weak (green) retroflection ($\pm 1\ \sigma$) used for the composite analyses. **(b) Salinity** in the subpolar North Atlantic (SPNA, dashed line) and **temperature** and salinity on the eastern American continental shelf (EACS, continuous lines), averaged over the top 500 m (boxes in Fig. 4a). Correlation coefficients with the retroflection index are respectively of -0.61, 0.54, and 0.61. **(c) Volume transport** across the SI (continuous line, on the Labrador Shelf) and HL (dashed line, on the Scotian Shelf) hydrographic sections (see supplementary figure S16 for location of the sections). **(d) Wind stress curl anomaly** averaged over the southern Labrador Shelf (box in Fig. 4b). **(e) Sea surface height** (SSH) averaged near the tip of the Grand Banks (box in Fig. 4c). **(f) Subpolar gyre area** based on the barotropic quasi-streamfunction of the velocity field over the top 1000 m of the ocean. In panels a, b, d and e, the green and red shading indicate the periods of, respectively, significantly weaker and stronger retroflection that are discussed in Section 2.1. In panels c and e, we shift the periods by 8 months, which gives the best lagged correlation and is the approximate advective time between the Labrador Shelf and the tip of the Grand Banks. C.c. denotes the correlation coefficient with the retroflection index. All variables are computed from the GLORYS12V1 reanalysis output, except for the wind stress curl, which is computed from the ERA-interim atmospheric reanalysis used to force GLORYS12V1. Seasonal variability is removed from all the variables using a one-year running mean.

associated with negative anomalies in the wind stress curl over the Labrador Shelf and the Grand Banks (Fig. 4b and 3d). These anomalies correspond to stronger zonal winds just north of the Grand Banks that push the water offshore and to a northward shift of the line of zero wind-stress-curl. Conversely, periods of weak retroflection correspond to positive anomalies in the wind stress curl over the Labrador Shelf (Fig. 4b), and to a southward shift in the line of zero wind-stress-curl. The southward shift connects regions of positive wind stress curl located over the Labrador Sea and the Scotian Shelf (Supplementary figure S2), reducing the offshore push of the winds. Wind seems to play a predominant role during the 1996-1999 weak retroflection period, when the correlation between the retroflection index and the Labrador Current strength is weak or absent (supplementary figure S6). The relationship between the retroflection of the Labrador Current and the wind stress curl has been previously highlighted for the winter winds by *Holliday et al.* (2020). The shifts in the wind patterns are related to variations in the atmospheric pressure field. During strong retroflection periods, we find that the north-south pressure difference across the jet stream is more pronounced (Fig. 4d). This sea-level pressure pattern reinforces the westerly winds, pushing the Labrador Current offshore, but also strengthening the gyre circulation. This pressure pattern is similar to a positive phase of the Arctic Oscillation (AO), but with a high pressure system closer to the Grand Banks. Whereas we find a significant negative correlation between the retroflection index and AO indices (-0.34, p0.0001), we find no correlation with the NAO index (supplementary figure S1) nor with the AMOC strength at 26°N (not shown).

2.3 Local forcing

The retroflection of the Labrador Current is also related to the configuration of the circulation at the tip of the Grand Banks, where the retroflection occurs. Along the Scotian and Grand Banks shelves, the retroflection index is positively correlated with the sea-surface height (SSH) anomaly (correlation coefficient of 0.62, $p < 0.0001$, Fig. 4c). A positive anomaly in SSH in that region is the signature of a northward shift in the position of the Gulf Stream. Thus, the retroflection is stronger when the Gulf Stream is closer to the Grand Banks. An important northward shift in the position of the Gulf Stream is detected in 2008 through a change point analysis in the SSH timeseries at the tip of the Grand Banks (*Neto et al.*, 2021), and coincides with a statistically significant shift in the retroflection index towards more positive phases over 2009-2015 (Fig. 3). This northward shift of the Gulf Stream has been argued to cause the retreat of the Labrador Current and the subsequent anomalously high temperatures (*Whitney et al.*, 2022; *Neto et al.*, 2021) and low oxygen concentrations (*Claret et al.*, 2018) observed in the Slope Sea and on the Scotian Shelf over that period.

The increased presence of the Gulf Stream at the tip of the Grand Banks in recent years has led to the hypothesis that interactions between the Labrador Current and the Gulf Stream could cause the retroflection (*Neto et al.*, 2021; *Townsend et al.*, 2015; *Urrego-Blanco and Sheng*, 2012). The Gulf Stream and Labrador Current are separated by a front, characterized by instabilities in the form of meanders and eddies (*Rossby*, 1999; *Brooks*, 1987). At the tip of the Grand Banks, cold cyclonic meanders and eddies generated by the tongue of Labrador Current Waters are frequent (supplementary figure S7). We find that, during events of strong retroflection, these cyclonic features divert virtual particles eastward (Fig. 5b), particularly below 300 m. During strong retroflection periods, enhanced interactions between the Gulf Stream and the Labrador Current produce more eddies and meanders, leading to more frequent trapping and diversion of the Labrador Current water by these cyclonic features. Diversion by cyclonic features is also visible observations (supplementary

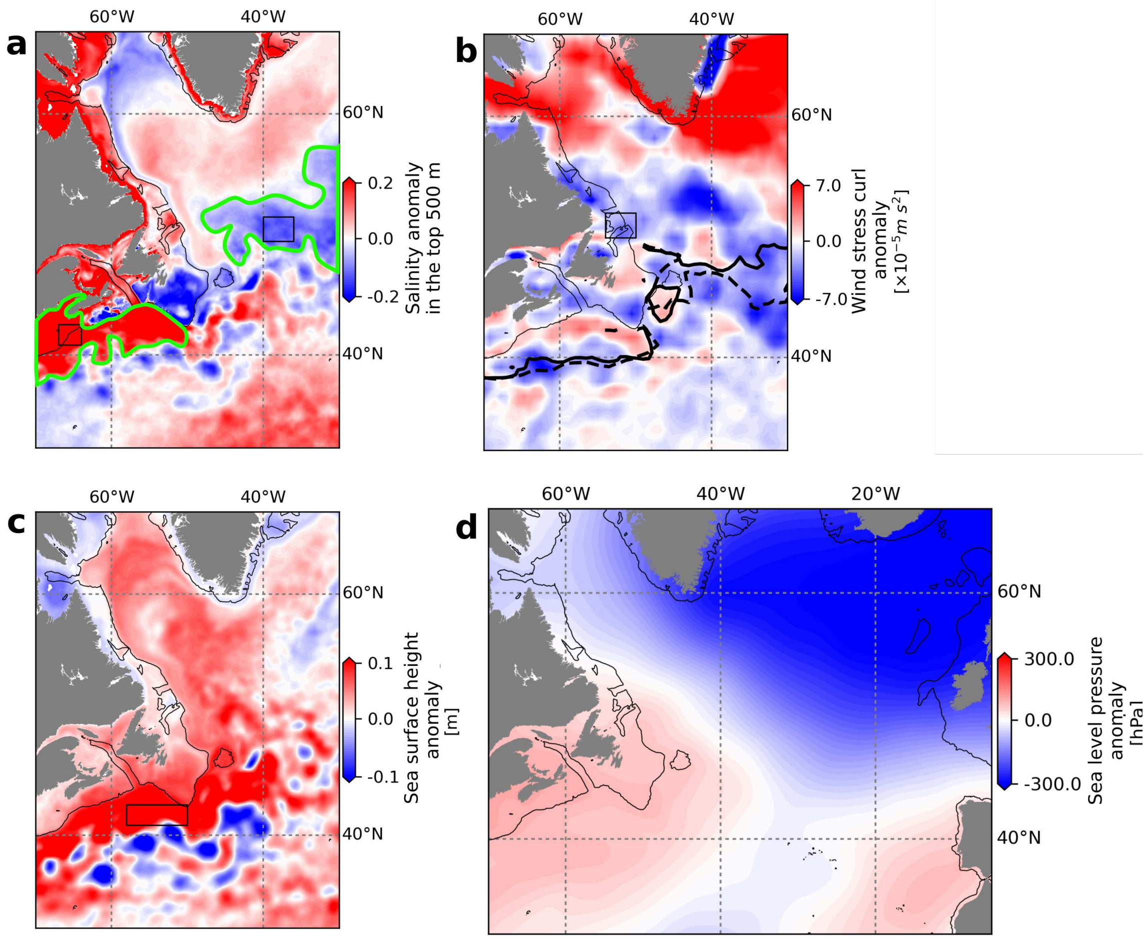

Figure 4: Difference between composites of strong and weak retroflection periods (strong minus weak) for **(a)** average salinity over the top 500 m of the ocean, **(b)** wind stress curl, **(c)** sea-surface height and **(d)** sea-level pressure (see Figs. S3 for maps of the composites). Years used in the composites are highlighted in green (weak retroflection) and red (strong retroflection) in Fig. 3. The black line delineates the 350 m isobath. The dashed and full thick lines in panel (b) show the position of the lines of zero wind-stress-curl during weak and strong retroflection periods, respectively. The green lines in (a) indicate regions of interest with strong difference between the composites. The boxes in panels (a-c) show the regions over which variables are averaged to produce the time series in Fig. 3. They are based on the zones of strongest correlations between the retroflection index and each field (supplementary figure S4).

figure S14). However, retroflection also occurs in the absence of such features, in more than a third of the identified events (Fig. 5a). We note that diversion of virtual particles by eddies and meanders at the tip of the Grand Banks is not a proof of the role of these circulation features in triggering the retroflection, as these circulation features can also result from the detachment of Labrador Current intrusions coming from the retroflection itself. In periods of weak retroflection, most virtual particles move westward in the absence of possibly diverting circulation features (Fig. 5c), although they sometimes do so even in their presence (Fig. 5d). These results suggest that whereas interactions with the Gulf Stream play a role in diverting the Labrador Current to the east, they are not a necessary condition for the retroflection to occur.

3 Discussion

There is no consensus yet on whether the retroflection of the Labrador Current is controlled by remote forcing, by local forcing (i.e. interactions with the Gulf Stream), or by a combination of both (see section 1). Based on correlations found between our retroflection index and the volume transport and the wind stress curl over the Labrador Shelf (Fig. 3 and 4), and considering the absence of a systematic effect of local circulation features at the tip of the Grand Banks on the retroflection (Fig. 5), we support the hypothesis that the retroflection is mostly controlled remotely, by wind and the large-scale ocean circulation in the North Atlantic, while the local forcing only plays a secondary role. Moreover, about a quarter of the retroflection takes place along Flemish Cap (Fig. 2), upstream of the tip of the Grand Banks, where there is no interaction between the Labrador Current and the Gulf Stream. An investigation of the leakiness of the Deep Western Boundary Current - the deep counterpart of the Labrador Current - in the Grand Banks area revealed that sharp bathymetric features, rather than interactions between the Deep Western Boundary Current and the NAC, cause that leakiness (*Solodoch et al.*, 2020).

No explanation has yet been proposed for the retroflection of the Labrador Current, in contrast to other retroflecting currents such as the Agulhas Current and the North Brazil Current (*Lutjeharms*, 2006; *De Ruijter*, 1982). We propose a scenario similar to that developed by *de Ruijter and Boudra* (1985) for the Agulhas Current to explain this retroflection. The Labrador Current is a western boundary current which hugs the coast under the Coriolis force. At the tip of the Grand Banks, the shelf edge takes an abrupt turn of more than 90° to the west (Fig. 1). Currents detach more easily from a cape when their velocity is higher (*Solodoch et al.*, 2020; *Bormans and Garrett*, 1989). For the Labrador Current, this detachment can occur for the fast ($\sim$0.3 - 0.5 m s^{-1}) offshore branches of the Labrador Current, while the slower inshore branches tend to follow the continental shelf (*de Ruijter and Boudra*, 1985). As a branch detaches from the shelf, it falls in free flow conditions, and overshoots the tip of the Grand Banks towards the south due to its accumulated inertia. This southward displacement comes with a decrease in the planetary vorticity of the flow, so that the relative vorticity must increase to conserve total potential vorticity (a process known as the β-compensation effect). This results in a cyclonic rotation of the flow and, hence, in a retroflection of the flow. According to this scenario, (1) a larger part of the Labrador Current would be prone to detach from the continental slope when the current is stronger, and (2) this stronger current, having a higher inertia upon reaching the tip of the Grand Banks, would overshoot further south, generating a stronger β-compensation effect (*de Ruijter and Boudra*, 1985). We therefore expect a tight link between the strength of the Labrador Current and its retroflection, in line with our results (Fig. 3).

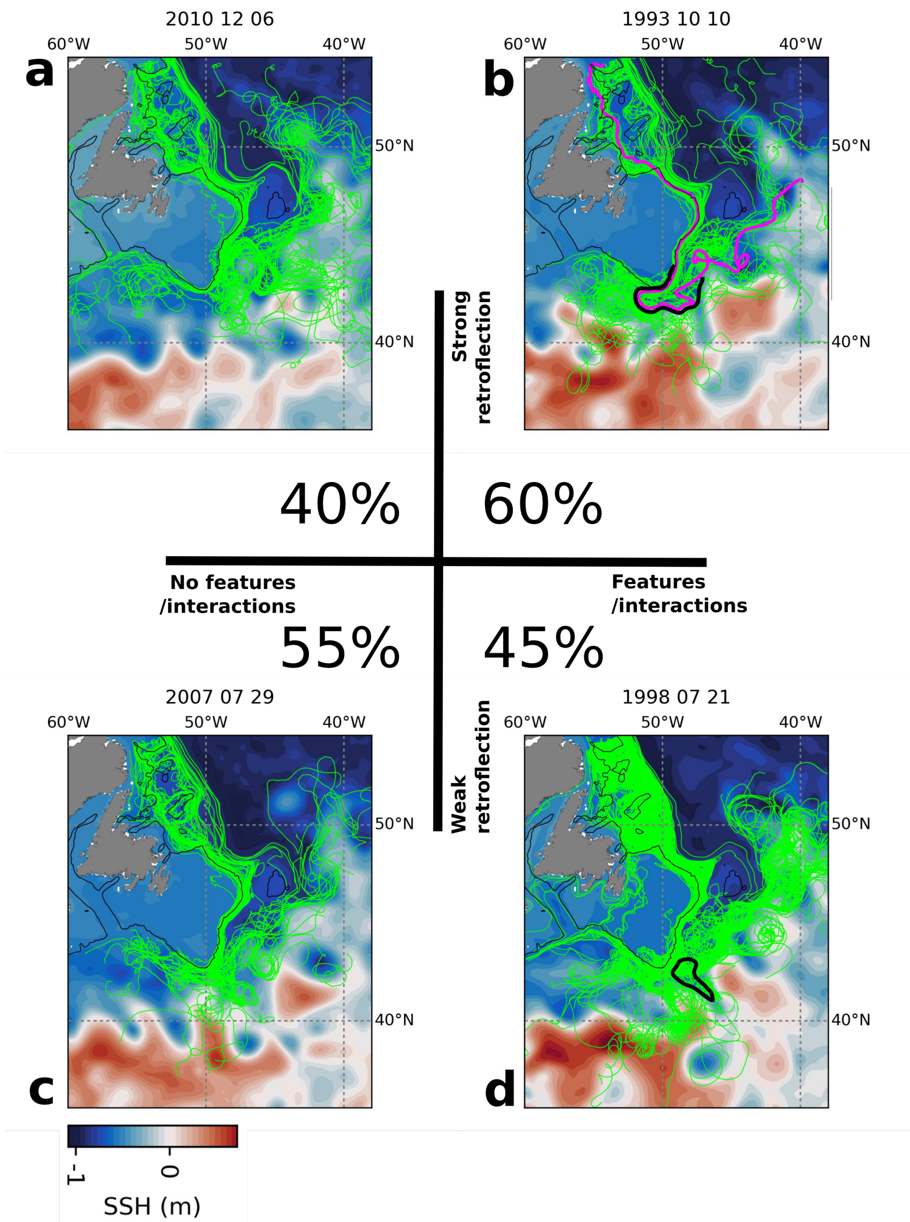

Figure 5: Assessment of the impact of cyclonic meanders and eddies at the tip of the Grand Banks on the intensity of the retroflection. Four cases are presented: absence (left) or presence (right) of cyclonic meanders or eddies in the context of strong (top) and weak (bottom) retroflection. Maps show the sea-surface height (background colors) and a subset of the trajectories coming in the vicinity of the Grand Banks (lime green) for specific events. In (b), the trajectory of a virtual particle showing an interaction with a cyclonic meander is highlighted in magenta. The thick black lines in (b) and (d) indicate the SSH contour of Labrador Current eddies or meanders detected using an eddy-detection tool (see section Method) near the tip of the Grand Banks. Percentages indicate the number of events falling into each category (see section 4.4).

Nevertheless, our results show that the current's strength does not explain all the variability in the retroflection. Winds also play a role, and both the winds' and current's strength are strongly related (*Zhang et al.*, 2016), through the subpolar gyre dynamics (*Böning et al.*, 2006). During strong retroflection periods, we find an increased meridional pressure gradient in the subpolar North Atlantic leading to stronger westerlies and a northward migration of the line of zero curl in wind stress. These anomalous winds push the Labrador Current offshore at the Grand Banks, encouraging the retroflection while strengthening and contracting the subpolar gyre (Fig. 6). In strengthening, the subpolar gyre in turn accelerates the Labrador Current, resulting in a stronger retroflection of the current, as discussed above. This retroflection occurs concurrently with the northward shift of the Gulf Stream, in response to the northward shift in the line of zero wind-stress-curl and the contraction of the subpolar gyre (*Peterson et al.*, 2017). The significant correlation between the position of the Gulf Stream and the retroflection of the Labrador Current (Fig. 4c) points to a large-scale adjustment of the circulation in the North Atlantic, instead of a blocking effect of the Gulf Stream forcing a retreat of the Labrador Current.

To conclude, our Lagrangian analysis highlights the major role of remote forcing through winds and gyre dynamics in controlling the retroflection of the Labrador Current (Fig. 6), pairing resullts of previous studies that suggested such a link (*Jutras et al.*, 2020; *Han et al.*, 2019; *Peterson et al.*, 2017; *New et al.*, 2021). We argue that the physical blocking of the Labrador Current by the Gulf Stream suggested by *Neto et al.* (2021); *Claret et al.* (2018); *Zhang et al.* (2016); *Urrego-Blanco and Sheng* (2012) needs to be considered within the context of the subpolar gyre dymanics, rather than as a local phenomenon. Local interactions with the Gulf Stream (*Neto*, 2021; *Townsend et al.*, 2015; *Urrego-Blanco and Sheng*, 2012) are found to play a secondary role in the retroflection.

The fact that the wind pattern as well as the strength of the Labrador Current are strongly correlated with the retroflection with a lag of a couple of months means that we can use these variables to monitor the export of the cold, fresh, and oxygen-rich Labrador waters towards the subpolar and coastal North Atlantic. Winds can be monitored from satellite data, while the Labrador Current strength can be monitored from the array of moorings located along the Labrador Shelf. Given the impact of the variability of the Labrador Current retroflection on the salinity, temperature, and oxygen and nutrient content in the identified export zones, this monitoring could serve to predict consequences on marine life, including fish stocks, and to set fishing quotas.

4 Method

4.1 GLORYS12V1 ocean reanalysis

We use the global 1/12° ocean physical reanalysis GLORYS12V1 (*Lellouche et al.*, 2018; *Fernandez and Lellouche*, 2018) from Copernicus Marine Environment Monitoring Service (CMEMS, `http://marine.copernicus.eu/,productnumberGLOBAL_REANALYSIS_PHY_001_030`). GLORYS12V1 is based on version 3.1 of the NEMO system (*Madec et al.*, 2019) and is run with version 2 of the Louvain-la-Neuve Ice elastic–viscous–plastic sea ice Model (LIM2) (*Fichefet and Maqueda*, 1997). Tides are not included. The model uses 50 levels on the vertical, with grid thicknesses ranging from 0.5 m at the surface to 160 m at 1000 m depth. The model is run on an Arakawa C grid at a nominal resolution of 1/12°, corresponding to $\sim$ 7 km at a latitude of 45°N. The reanalysis covers the period from 1993 to 2018. It is forced with the 3h/24h atmospheric reanalysis ERA-Interim (*Dee et al.*,

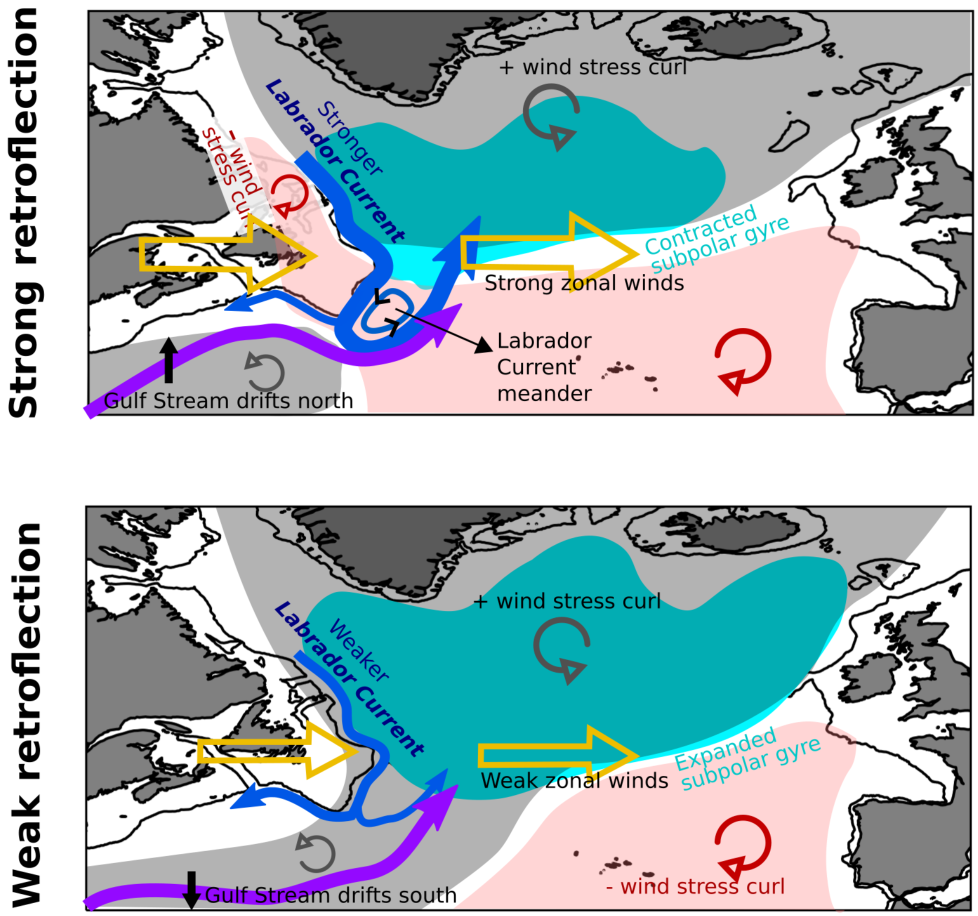

Figure 6: Schematic of the oceanic and atmospheric states during strong (top) and weak (bottom) retroflection of the Labrador Current. During strong retroflection, negative wind stress curl anomalies over the Labrador Shelf reinforce zonal winds, the subpolar gyre is contracted, the Labrador Current is accelerated, the Gulf Stream shifts north, and Labrador Current meanders and eddies at the tip of the Grand Banks deflect some waters towards the east. During weak retroflection, regions of positive wind stress curl anomalies connect over the Grand Banks area, the zonal winds are weaker, the subpolar gyre expands, the Labrador Current weakens, and the Gulf Stream shifts south. The black lines delineates the 350-m isobath. Part of the schematic is inspired from *Holliday et al.* (2020).

2011). The bathymetry is downscaled from a resolution of 1/60° or ∼1 km at 45°N in the deep ocean (ETOPO1 from NOAA) and of 1/120° or ∼1 km on the coast (GEBCO-08). The assimilated data comprises 1/4° NOAA sea surface temperature (SST), altimetry-derived surface level anomaly (SLA) from AVISO, in situ temperature and salinity profiles from the CMEMS CORAv4.1 database, and CERSAT sea-ice concentrations (*Fernandez and Lellouche*, 2018). Observations are assimilated using a reduced-order Kalman filter with a 3-D multivariate modal decomposition of the forecast error and a 7-day assimilation cycle (*Lellouche et al.*, 2013). We use the daily outputs regrided on a centered grid.

GLORYS12V1 provides a good representation of ocean circulation, with a slight overestimation of the intensity of western boundary currents (*Buongiorno Nardelli*, 2020; *Drévillon et al.*, 2018). It reproduces the variability of the AMOC as measured at the RAPID mooring array (*Drévillon et al.*, 2018). Models with similar spatial resolutions as GLORYS12V1 have been shown to reproduce well the location and transport of the Labrador Current (*Florindo-López et al.*, 2020), the physics and biogeochemistry of the eastern American shelf (*Laurent et al.*, 2020), and the location of the Gulf Stream (*Saba et al.*, 2016). A comparison with observations shows that the location and timing of fronts and eddies are well represented in GLORYS12V1, as well as the main circulation features of the Labrador Current, with an underestimation of velocity of the Labrador shelf-break jet (supplementary material C). To limit the analysis to the Labrador Current and exclude the Deep Western Boundary Current (DWBC), we do not consider waters with practical salinities $S_P < 34.8$ (see Fig. S11a; *Loder et al.*, 1998, *Myers, P., personal communication, 2021*).

4.2 Observational datasets

We compare the Lagrangian trajectories of virtual particles with recordings of observational instruments, namely Argo floats, RAFOS and SOFAR floats, and surface drifters. Argo floats are autonomous profilers that drift passively with ocean currents at a parking depth (typically 1000 meters), and profile temperature, salinity and pressure down to approximately two kilometers every 10 days. We select the floats that cross the hydrographic line (56.7°W, 53°N) – (50°W, 54.9°N) and enter the Grand Banks area as defined by the (55°W; 43°W) – (45°N; 50°N) box. The northernmost line extends more offshore than that used to initiate our virtual particles (Fig. 1b,c) to account for the fact that Argo floats drift deeper than the virtual particles, hence further offshore on the continental slope. This provides us with a dataset of 64 Argo floats that drift within the Labrador Current in the proximity of the Grand Banks, between 2001 and 2019.

The RAFOS and SOFAR (SOund Fixing And Ranging channel) subsurface floats are compiled from 52 experiments by the WOCE Subsurface Float Data Assembly Center. These floats drift at depths between 500 meters and one kilometer. The position of these floats is retrieved via acoustic methods. RAFOS floats recognize 'pongs' emitted by moorings, and SOFAR floats emit 'pongs' retrieved by moorings. We identify 50 drifters corresponding to the same criteria as the Argo floats, between 2003 and 2007.

Surface drifters are satellite-tracked buoys deployed as part of the Global Drifter Program. The buoys drift at the surface of the ocean and are equipped with 15 m or 1 m drogues. We select the drifters that move southward through a box located near the Grand Banks (55°W - 41°W and 45°N - 50°N). Based on these criteria, we identify 79 drifters between 2000 and 2018. To separate the floats and drifters that retroflect from those that go west, we determine if the platforms cross the 54th meridian south of the Grand Banks (pink line in Fig. 1c).

4.3 Index of retroflection of the Labrador Current

A retroflection index is derived from Lagrangian tracking experiments of virtual passive particles. The experiments are carried with the OceanParcels (Probably A Really Computationally Efficient Lagrangian Simulator) tool for Python (`http://oceanparcels.org`, *Delandmeter and Van Sebille* (2019)), using the daily horizontal velocities from GLORYS12V1 and the reconstructed vertical velocities obtained by considering the non-divergence of the flow and the change in sea surface height. Virtual particles are seeded along the (53°N, 56.7°W)–(54.3°N, 52.0°W) line (Fig. 1) every 1/12° in the horizontal and every 10 m in the vertical, for a total of 966 particles per seeding event. This number is sufficient, as increasing it does not significantly alter the percentage of particles being retroflected or going westward. Particles are released every week from 01-01-1993 to 01-01-2015 and are tracked for three years, with a 10-minute time step. After three years, the particles have either reached the boundaries of the domain or have moved far from the Grand Banks.

Few particles circumnavigate the Grand Banks and reach the Scotian Shelf and Slope Sea, in agreement with results of other modelling (*Neto et al.* (2021), *Myers, P., personal communication, 2021*) and float-based (*Lavender et al.*, 2005; *Fischer and Schott*, 2002; *Reverdin et al.*, 2003) studies, as well as with our own analysis of floats and drifters trajectories (Fig. 1c). Nonetheless, to verify whether the forward tracking experiments miss a contribution from the Labrador Current to the Slope Sea, we carried out a backtracking experiment in which particles are initialized on the Scotian Shelf and Slope Sea. The experiment confirms that less than 20% of the particles reaching the Scotian Shelf and Slope Sea originate from these regions, and that the region is mostly supplied by water coming from the North Atlantic Ocean or by outflow from the Laurentian Channel.

We define a retroflection index by first counting the number of particles passing daily through hydrographic sections located on the Labrador Shelf and on the Scotian Shelf (pink lines on Fig. 1a). The index covers the 1993 to 2015 period. The Lagrangian retroflection index is then computed from the difference between the number of particles crossing these two sections, and is smoothed with a 12-month rolling average that removes high frequencies (for the spectrum of the retroflection index, see supplementary figure S12b). The index is then normalized from -1 to 1, and the average over the whole period (1993-2015) is removed. A detrended index is also defined, by removing the statistically significant positive trend in the retroflection index.

4.4 Mechanisms controlling the retroflection

To identify the mechanisms controlling the retroflection, we produce correlation and composite maps between the retroflection index and variables representative of the atmospheric, climatic and oceanic state. The composite maps are computed from periods with anomalies greater than one standard deviation from the mean in the detrended retroflection index. The detrended index captures the interannual variability of the retroflection and allows us to examine the mechanisms controlling the retroflection at that time scale. We use the daily salinity, temperature and sea surface height outputs from GLORYS12V1, and compute the daily volume transport, density and pressure gradients from the available outputs. The daily time series of the investigated variables are smoothed with a 12-months rolling average. The wind and the sea level pressure are taken from the ERA-Interim atmospheric reanalysis, used to force GLORYS12V1. In addition to the variables presented in this paper, variables showing no correlation with the retroflection are discussed in supplementary material B. We compute different climate indices (see section 2.2). The NAO index is computed from the first principal component of the sea level pressure anomaly in the region formed by (20°N,80°N)–(90°W,40°E) (*Hurrell et al.*, 2003), and the AO index from the 20°N–80°N region. The AMOC transport at 26°N is computed by the CMEMS team. We define an index of the subpolar gyre extent, based on the barotropic quasi-steamfunction of velocity integrated over the top 1000 m of the ocean. The subpolar gyre index is calculated as the area of a fixed closed contour of this streamfunction that encloses the subpolar gyre (supplementary figure S5), calculated for each month.

We investigate the influence of eddies and meanders at the tip of the Grand Banks on the trajectories of the virtual particles in every individual weak and strong retroflection event (± 1 standard deviation from the mean), based on the unfiltered retroflection index. We do so by inspecting maps of the trajectories of virtual particles passing the Grand Banks area during the events, also showing the SSH field at the time of the passage (Fig. 5). We then examine whether there is or not an eddy or a meander near the tip of the Grand Banks collocated with particles deviated to the east. Eddies are also detected using a Python package based on the Okubo-Weiss (OW) parameter, following *Oliver et al.* (2015) and *Chelton et al.* (2011). We define the zone of interest at the tip of the Grand Banks as the (55°E, 45°E) – (38°N – 45°N) box. The OW parameter is computed at a depth of 185 m, as it offers the best detection performance. The OW threshold is set to -0.35, and eddies smaller than 190 pixels on the $1/12^\circ$ grid are not considered.

Data availability

The Lagrangian tracking experiments were performed using ocean velocity output from GLORYS12V1 and the OceanParcels particle tracking tool. The eddy detection Python package is available at `https://github.com/jk-rieck/eddytools`. Model output from GLORYS12V1 can be downloaded from the Copernicus Marine Environment Monitoring Service (CMEMS) website: `https://resources.marine.copernicus.eu/product-detail/GLOBAL_MULTIYEAR_PHY_001_030/INFORMATION`. The OceanParcels Python package can be found at `https://oceanparcels.org/`. The ERA-interim atmospheric reanalysis can be downloaded from `https://www.ecmwf.int/en/forecasts/datasets/reanalysis-datasets/era-interim`. The RAFOS/SOFAR float data can be downloaded from `https://www.aoml.noaa.gov/phod/float_traj/`. The Argo data were collected and made freely available by the International Argo Program and the national programs that contribute to it (`https://argo.ucsd.edu`, `https://www.ocean-ops.org`). The Argo Program is part of the Global Ocean Observing System. The surface drifter data from the Global Drifter Program is available at `ftp.aoml.noaa.gov/phod/pub/buoydata`.

Acknowledgments

The Natural Sciences and Engineering Research Council of Canada (NSERC), the Fonds de recherche du Québec - Nature et technologie (FRQNT) and Ouranos funded M.J. through doctoral scholarships. This research was also funded by NSERC through Discovery grants to A.M. and NSERC Accelerator Supplements to C.O.D. M.J. and C.O.D. also wish to acknowledge the support of the Québec-Océan research network. The ADCP data used in these analyses were collected as part of a long-term observation program, the Atlantic Zone Monitoring Program. Many scientists have contributed to the collection, quality assurance and analyses that resulted in making these data available for research, as have the officers and crews of Fisheries and Oceans Canada's research vessels. M.J. would also like to thank N. Foukal for discussions on the subpolar gyre, J.K. Rieck for insightful ideas, and P. Myers for discussions on the Labrador Current and for sharing model outputs.

Author contribution

M.J. led the development of the study, performed the analyses, produced the figures and was lead writer of the text. C.O.D. contributed to the development of the study, the interpretation of the results and the writing of the manuscript. L.T. performed the analyses of the observational dataset and produced the corresponding figures and text. A.M. and C.O.D. revised the manuscript.

References

Böning, C. W., M. Scheinert, J. Dengg, A. Biastoch, and A. Funk, Decadal variability of subpolar gyre transport and its reverberation in the North Atlantic overturning, *Geophysical Research Letters*, *33*(21), 1–5, doi:10.1029/2006GL026906, 2006.

Böning, C. W., E. Behrens, A. Biastoch, K. Getzlaff, and J. L. Bamber, Emerging impact of Greenland meltwater on deepwater formation in the North Atlantic Ocean, *Nature Geoscience*, *9*(7), 523–527, doi:10.1038/ngeo2740, 2016.

Bormans, M., and C. Garrett, A simple criterion for gyre formation by the surface outflow from a strait, with application to the alboran sea, *Journal of Geophysical Research: Oceans*, *94*(C9), 12,637–12,644, doi:10.1029/JC094iC09p12637, 1989.

Brooks, D. A., The Influence of Warm-Core Rings on Slope Water Entering the Gulf of Maine, *Journal of Geophysical Research*, *92*(C8), 8183–8196, 1987.

Buongiorno Nardelli, B., A multi-year time series of observation-based 3D horizontal and vertical quasi-geostrophic global ocean currents, *Earth System Science Data*, *12*(3), 1711–1723, doi:10.5194/essd-12-1711-2020, 2020.

Carr, M.-e., and H. T. Rossby, Pathways of the North Current from surface drifters and subsurface floats, *Journal of Geophysical Research*, *106*(C3), 4405–4419, 2001.

Chabot, D., and J. D. Dutil, Reduced growth of Atlantic cod in non-lethal hypoxic conditions, *Journal of Fish Biology*, *55*(3), 472–491, doi:10.1006/jfbi.1999.1005, 1999.

Chelton, D. B., M. G. Schlax, and R. M. Samelson, Global observations of nonlinear mesoscale eddies, *Progress in Oceanography*, *91*(2), 167–216, doi:10.1016/j.pocean.2011.01.002, 2011.

Chen, Z., Y. O. Kwon, K. Chen, P. S. Fratantoni, G. Gawarkiewicz, and T. M. Joyce, Long-Term SST Variability on the Northwest Atlantic Continental Shelf and Slope, *Geophysical Research Letters*, *47*(1), 1–11, doi:10.1029/2019GL085455, 2020.

Claret, M., E. D. Galbraith, J. B. Palter, D. Bianchi, K. Fennel, D. Gilbert, and J. P. Dunne, Rapid coastal deoxygenation due to ocean circulation shift in the northwest Atlantic, *Nature Climate Change*, *8*, doi:10.1038/s41558-018-0263-1, 2018.

De Ruijter, W., Asymptotic Analysis of the Agulhas and Brazil Current Systems, *Journal of Physical Oceanography*, *12*, 361–373, 1982.

de Ruijter, W. P., and D. B. Boudra, The wind-driven circulation in the South Atlantic-Indian Ocean-I. Numerical experiments in a one-layer model, *Deep Sea Research Part A, Oceanographic Research Papers*, *32*(5), 557–574, doi:10.1016/0198-0149(85)90044-5, 1985.

Dee, D. P., et al., The ERA-Interim reanalysis: Configuration and performance of the data assimilation system, *Quarterly Journal of the Royal Meteorological Society*, *137*(656), 553–597, doi:10.1002/qj.828, 2011.

Delandmeter, P., and E. Van Sebille, The Parcels v2.0 Lagrangian framework: New field interpolation schemes, *Geoscientific Model Development*, *12*(8), 3571–3584, doi:10.5194/gmd-12-3571-2019, 2019.

Drévillon, M., C. Régnier, J.-M. Lellouche, G. Garric, C. Bricaud, and O. Hernandez, Quality Information Document for Global Ocean Reanalysis Products GLOBAL-REANALYSIS-PHY-001-030, *Tech. Rep. 1.2*, Copernicus Marine Environment Monitoring Service, 2018.

Fernandez, E., and J.-M. Lellouche, Product User Manual for the Global Ocean Physcal Reanalysis Product GLORYS12V1, *Tech. Rep. April*, 2018.

Fichefet, T., and M. A. Maqueda, Sensitivity of a global sea ice model to the treatment of ice thermodynamics and dynamics, *Journal of Geophysical Research: Oceans*, *102*(C6), 12,609–12,646, doi:10.1029/97JC00480, 1997.

Fischer, J., and F. A. Schott, Labrador Sea Water tracked by profiling floats - From the boundary current into the Open North Atlantic, *Journal of Physical Oceanography*, *32*(2), 573–584, doi:10.1175/1520-0485(2002)032<0573:LSWTBP>2.0.CO;2, 2002.

Florindo-López, C., S. Bacon, Y. Aksenov, L. Chafik, E. Colbourne, N. Penny Holliday, and N. P. Holliday, Arctic Ocean and Hudson Bay Freshwater Exports : New Estimates from 7 Decades of Hydrographic Surveys on the Labrador Shelf, *Journal of Climate*, *33*(20), 1–62, doi:10.1175/jcli-d-19-0083.1, 2020.

Fratantoni, P. S., and M. S. McCartney, Freshwater export from the Labrador Current to the North Atlantic Current at the Tail of the Grand Banks of Newfoundland, *Deep-Sea Research Part I: Oceanographic Research Papers*, *57*(2), 258–283, doi:10.1016/j.dsr.2009.11.006, 2010.

Fratantoni, P. S., and R. S. Pickart, The western North Atlantic shelfbreak current system in summer, *Journal of Physical Oceanography*, *37*(10), 2509–2533, doi:10.1175/JPO3123.1, 2007.

Gilbert, D., B. B. Sundby, C. Gobeil, A. Mucci, and G.-H. Tremblay, A seventy-two-year record of diminishing deep-water oxygen in the St. Lawrence estuary: The northwest Atlantic connection, *Limnology and Oceanography*, *50*(5), 1654–1666, 2005.

Han, G., Z. Ma, and N. Chen, Ocean climate variability off Newfoundland and Labrador over 1979–2010: A modelling approach, *Ocean Modelling*, *144*(October), 101,505, doi:10.1016/j.ocemod.2019.101505, 2019.

Holliday, N. P., et al., Ocean circulation causes the largest freshening event for 120 years in eastern subpolar North Atlantic, *Nature Communications*, *11*(1), doi:10.1038/s41467-020-14474-y, 2020.

Hurrell, J. W., Y. Kushnir, G. Ottersen, and M. Visbeck, An overview of the North Atlantic Oscillation, in *The North Atlantic Oscillation Climatic Significance and Environmental Impact*, edited by J. W. Hurrell, Y. Kushnir, G. Ottersen, and M. Visbeck, chap. 1, pp. 1–36, American Geophysical Union, 2003.

Jutras, M., N. Planat, and C. O. Dufour, Unsupervised clustering of oceanic Lagrangian particles: identification of the main pathways of the Labrador Current.

Jutras, M., C. O. Dufour, A. Mucci, F. Cyr, and D. Gilbert, Temporal Changes in the Causes of the Observed Oxygen Decline in the St. Lawrence Estuary, *Journal of Geophysical Research: Oceans*, *125*(12), 1–20, doi:10.1029/2020JC016577, 2020.

Laurent, A., K. Fennel, and A. Kuhn, An observation-based evaluation and ranking of historical Earth System Model simulations for regional downscaling in the northwest North Atlantic Ocean, *Biogeosciences Discussions*, (March), 1–36, doi:10.5194/bg-2020-265, 2020.

Lavender, K. L., W. Brechner Owens, and R. E. Davis, The mid-depth circulation of the subpolar North Atlantic Ocean as measured by subsurface floats, *Deep-Sea Research Part I: Oceanographic Research Papers*, *52*(5), 767–785, doi:10.1016/j.dsr.2004.12.007, 2005.

Lellouche, J. M., et al., Evaluation of global monitoring and forecasting systems at Mercator Océan, *Ocean Science*, *9*(1), 57–81, doi:10.5194/os-9-57-2013, 2013.

Lellouche, J.-M., et al., Recent updates to the Copernicus Marine Service global ocean monitoring and forecasting real-time 1/12° high-resolution system, *Ocean Science*, *14*(5), 1093–1126, doi:10.5194/os-14-1093-2018, 2018.

Loder, J. W., B. D. Petrie, and G. Gawarkiewicz, The coastal ocean off northeastern North America: a large-scale view, in *The Sea*, vol. 11, chap. 5, pp. 105–133, 1998.

Luo, Y., M. D. Prater, E. G. Durbin, and L. M. Rothstein, Changes in the Northwest Atlantic circulation for the 1992-95 high NAO period from a numerical model, *Continental Shelf Research*, *26*(14), 1617–1635, doi:10.1016/j.csr.2006.05.006, 2006.

Lutjeharms, J. R., The Agulhas Current retroflection, in *The Agulhas Current*, chap. 6, pp. 151–207, Springer, Berlin, Heidelberg, doi:10.1007/3-540-37212-1_6, 2006.

Madec, G., et al., NEMO ocean engine (Version v4. 0), 2019.

Mertens, C., M. Rhein, M. Walter, C. W. Boning, E. Behrens, D. Kieke, R. Steinfeldt, and U. Stoeber, Circulation and transports in the Newfoundland Basin, western subpolar North Atlantic, *Journal of Geophysical Research : Oceans*, *119*, 7772–7793, doi:10.1038/175238c0, 2014.

Mills, K. E., et al., Fisheries management in a changing climate: Lessons from the 2012 ocean heat wave in the Northwest Atlantic, *Oceanography*, *26*(2), doi:10.5670/oceanog.2013.27, 2013.

Neto, A. G., North Atlantic on the Edge: Ocean Circulation Through Gateways at the Subpolar-Subtropical Boundary, Ph.D. thesis, University of Rhode Island, 2021.

Neto, A. G., J. A. Langan, and J. B. Palter, Changes in the Gulf Stream precede rapid warming of the Northwest Atlantic Shelf, *Nature Communications Earth Environment*, *2*(74), doi:10.1038/s43247-021-00143-5, 2021.

New, A., D. A. Smeed, A. Czaja, A. T. Blaker, J. V. Mecking, J. P. Mathews, A. S. Franks, and A. Sanchez-Franks, Labrador Slope Water Connects the Subarctic with the Gulf Stream, *Environmental Research Letters*, *16*(8), 084,019, doi:10.1088/1748-9326/ac1293, 2021.

Oliver, E. C., T. J. O'Kane, and N. J. Holbrook, Projected changes to Tasman Sea eddies in a future climate, *Journal of Geophysical Research: Oceans*, *120*, 7150–7165, doi:10.1002/2015JC011107. Received, 2015.

Peña-Molino, B., and T. M. Joyce, Variability in the Slope Water and its relation to the Gulf Stream path, *Geophysical Research Letters*, *35*(3), 1–5, doi:10.1029/2007GL032183, 2008.

Pérez-Brunius, P., T. Rossby, and D. R. Watts, Absolute transports of mass and temperature for the North Atlantic Current-subpolar front system, *Journal of Physical Oceanography*, *34*(8), 1870–1883, doi:10.1175/1520-0485(2004)034<1870:ATOMAT>2.0.CO;2, 2004.

Pershing, A. J., et al., Oceanographic Responses to Climate in the Northwest Atlantic, *Oceanography*, *14*(3), 76–82, doi:10.1139/f93-270, 2001.

Pershing, A. J., et al., Slow adaptation in the face of rapid warming leads to collapse of the Gulf of Maine cod fishery, *Science*, *352*(6284), 423, doi:10.1126/science.aae0463, 2016.

Peterson, I., B. Greenan, D. Gilbert, and D. Hebert, Variability and wind forcing of ocean temperature and thermal fronts in the Slope Water region of the Northwest Atlantic, *Journal of Geophysical Research: Oceans*, *122*, 7325–7343, doi:10.1002/2016JC012335.Received, 2017.

Petrie, B. D., and K. F. Drinkwater, Temperature and Salinity Variability on the Scotian Shelf and in the Gulf of Maine 1945-1990, *Journal of Geophysical Research*, *98*(C11), 20,079–20,089, 1993.

Pickart, R. S., M. A. Spall, and J. R. N. Lazier, Mid-depth ventilation in the western boundary current system of the sub-polar gyre, *Deep-Sea Research Part I: Oceanographic Research Papers*, *44*(6), 1025–1054, doi:10.1016/S0967-0637(96)00122-7, 1997.

Pickart, R. S., T. K. McKee, D. J. Torres, and S. A. Harrington, Mean Structure and Interannual Variability of the Slopewater System South of Newfoundland, *Journal of Physical Oceanography*, *29*(10), 2541–2558, doi:10.1175/1520-0485(1999)029<2541:MSAIVO>2.0.CO;2, 1999.

Poitevin, P., J. Thebault, V. Siebert, S. Donnet, P. Archambault, J. Doré, L. Chauvaud, and P. Lazure, Growth response of Arctica islandica to North Atlantic oceanographic conditions since 1850, *Frontiers in Marine Science*, *6*, 1–14, doi:10.3389/fmars.2019.00483, 2019.

Reverdin, G., P. P. Niiler, and H. Valdimarsson, North Atlantic Ocean surface currents, *Journal of Geophysical Research*, *108*(1), doi:10.1029/2001jc001020, 2003.

Rossby, T., On gyre interactions, *Deep-Sea Research Part II: Topical Studies in Oceanography*, *46*(1-2), 139–164, doi:10.1016/S0967-0645(98)00095-2, 1999.

Saba, V. S., et al., Enhanced warming of the Northwest Atlantic Ocean under climate change, *Journal of Geophysical Research: Oceans*, *121*, 118–132, 2016.

Solodoch, A., J. C. McWilliams, A. L. Stewart, J. Gula, and L. Renault, Why does the deep western boundary current "leak" around flemish cap?, *Journal of Physical Oceanography*, *50*(7), 1989–2016, doi:10.1175/JPO-D-19-0247.1, 2020.

Stendardo, I., M. Rhein, and R. Steinfeldt, The North Atlantic Current and its volume and freshwater transports in the subpolar North Atlantic , time period 1993 - 2016, *Journal of Geophysical Research : Oceans*, *125*(e2020JC016065), doi:10.1029/2020JC016065, 2020.

Townsend, D. W., N. R. Pettigrew, M. A. Thomas, M. G. Neary, D. J. Mcgillicuddy, and J. O. Donnell, Water masses and nutrient fluxes to the Gulf of Maine, *Journal of Marine Research*, *73*, 93–122, doi:10.1038/141548c0, 2015.

Urrego-Blanco, J., and J. Sheng, Interannual variability of the circulation over the eastern Canadian shelf, *Atmosphere - Ocean*, *50*(3), 277–300, doi:10.1080/07055900.2012.680430, 2012.

Wang, Z., Y. Lu, F. Dupont, J. W. Loder, C. Hannah, and D. G. Wright, Variability of sea surface height and circulation in the North Atlantic: Forcing mechanisms and linkages, *Progress in Oceanography*, *132*, 273–286, doi:10.1016/j.pocean.2013.11.004, 2015.

Whitney, N. M., A. D. Wanamaker, C. C. Ummenhofer, N. Cresswell-clay, K. J. Kreutz, and B. J. Johnson, Rapid 20th century warming reverses 900-year cooling in the Gulf of Maine, *Nature Communications Earth Environment*, *3*(179), 1–15, doi:10.1038/s43247-022-00504-8, 2022.

Wu, Y., C. Tang, and C. Hannah, The circulation of eastern Canadian seas, *Progress in Oceanography*, *106*, 28–48, doi:10.1016/j.pocean.2012.06.005, 2012.

Zhang, S., Y. Luo, L. M. Rothstein, and K. Gao, A numerical investigation of the interannual-to-interpentadal variability of the along-shelf transport in the Middle Atlantic Bight, *Continental Shelf Research*, *122*, 14–28, doi:10.1016/j.csr.2016.03.022, 2016.

Supplementary Files

This is a list of supplementary files associated with this preprint. Click to download.

- Jutrassupplementarymaterial.pdf